JOURNAL OF CATALYSIS 59, 79–99 (1979)

Aspects of Selective Oxidation and Ammoxidation Mechanisms over Bismuth Molybdate Catalysts[1]

JAMES D. BURRINGTON AND ROBERT K. GRASSELLI

Department of Research and Development, The Standard Oil Co. (Ohio), Cleveland, Ohio 44128

Received August 10, 1978; revised January 9, 1979

The interaction of allyl radicals, generated *in situ* by thermal nitrogen extrusion from 3,3′-azopropene, was studied at 320°C. The catalyst systems were MoO_3, $Bi_2O_3 \cdot nMoO_3$ (where $n = 1$, 2, and 3), a multicomponent Bi-molybdate, and Bi_2O_3. Allyl radicals gave significantly more byproducts (e.g., CO_2, acetaldehyde, benzene) than did allyl iodide or propylene under corresponding reaction conditions. When allyl radicals were generated from azopropene over MoO_3, and in the presence of ammonia, substantial yields of acrylonitrile were obtained. In the absence of ammonia, acrolein was the major useful product. The results for propylene oxidation and ammoxidation over Bi-molybdates are interpreted in terms of a concerted chemisorption, α-hydrogen abstraction mechanism, with subsequent oxygen (or NH) insertion, which does not proceed via a free allyl radical as the major pathway. Allyl radicals can, however, favorably compete with ammonia for oxygen (or NH) insertion sites over MoO_3 at 320°C. The proposed mechanism involves the formation of a π-allylic Mo(V) intermediate as the rate-determining step, in rapid equilibrium with a σ-bonded Mo(V) ester, the acrolein precursor. Acrylonitrile formation is explained by reaction of the initially formed π-allylic intermediate with ammonia, loss of water, and subsequent H-abstraction from the thus formed σ-bonded Mo(V) amide.

INTRODUCTION

It is generally accepted that the rate determining step in the selective oxidation of propylene is the abstraction of a α-hydrogen to form an allylic intermediate (*1*), a process which equilibrates the two ends of carbon moiety (*1d*). While the exact nature of this intermediate has been a subject of controversy, it is generally agreed that the oxidation state more closely resembles that of an allyl radical than an allyl cation or anion (*2*). Studies of selective oxidation of allyl halides have been interpreted as consistent with these results (*3*).

With regard to these latter studies, Haber and co-workers (*3a*) have found that allyl "radicals," generated from thermal homolytic C–I bond cleavage in allyl iodide, are converted to acrolein over MoO_3 with almost 100% selectivity. This result is in accord with their proposal that oxygen polyhedra associated with bismuth are responsible for α-hydrogen abstraction, forming the allyl species, while oxygens associated with molybdenum are responsible for oxygen insertion into the allylic intermediate. Similar results for allyl bromide have also been reported (3*b*).

However, it is not apparent that the interaction of allyl iodide with MoO_3 is proceeding via allyl radicals, as opposed to chemisorption of allyl iodide, followed by

---

[1] Presented at the Fourth International Roermond Conference on Catalysis, Netherlands, July 7, 1978.

0021-9517/79/100079-21$02.00/0

homolytic C–I cleavage and subsequent oxygen insertion. The latter mechanism seems more likely when one considers that, in the thermal decomposition of allyl iodide at 320°C, the total conversion is only about 25%, whereas, at the same temperature over MoO_3, 100% conversion is effected. Since the thermal reaction involves homolytic C–I cleavage to form allyl radicals in the rate-determining step, the faster reaction over MoO_3 must mean that a process having lower activation energy than homolytic C–I cleavage is occurring.

We propose that allyl iodide is chemisorbed on MoO_3, reducing the activation energy for homolytic C–I cleavage to form a Mo–π allylic species, which then undergoes oxygen insertion. Thus, free allyl radicals are probably not involved in the reaction of allyl iodide and MoO_3 at 320°C.

To provide stronger evidence concerning the nature of the allylic intermediate, we have generated allyl radicals over MoO_3 by the thermal extrusion of nitrogen from 3,3′-azopropene **1** [Eq. (1)]. This compound has been well studied and is

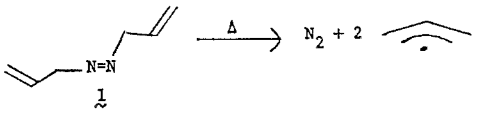

(1)

known to be a very clean source of allyl radicals (*4*). The activation energy for Eq. (1) is 36.1 kcal/mole, compared to 43.5 kcal/mole for allyl iodide decomposition, allowing a more facile generation of allyl radicals.

Mechanistic information concerning the role of allyl radicals in ammoxidation is also accessible by studying the decomposition of **1** over Bi/Mo-containing catalysts in the presence of ammonia. Such experiments at 320°C would provide insight into the ammonia deactivation of these catalysts toward propylene at this temperature.

The aims of this study, then are first to investigate the products of reaction of allyl radicals, generated *in situ* from thermolysis of **1** over MoO_3, $Bi_2O_3 \cdot 3MoO_3$, $Bi_2O_3 \cdot 2MoO_3$, $Bi_2O_3 \cdot MoO_3$, a multicomponent Bi-molybdate, and Bi_2O_3, to compare these results with those for allyl iodide and propylene under the same conditions, and to study the reaction of allyl radicals in the presence of ammonia over MoO_3 at 320°C.

EXPERIMENTAL

Allyl iodide (Eastman, 95%) was purified by the method of Sibbet and Noyes (*5*). Azopropene was prepared by the method of Al-Sader and Crawford (*4*) and purified by preparative gas chromatography using 10% UC on LB550-X on Flouropak 80 at 90°C (*6*). Catalysts were prepared as shown in Table 1.

All experiments were performed by the pulse method. A microsyringe was used to introduce samples of neat or diluted (in *n*-octane) allyl iodide and azopropene (1) directly onto the hot catalyst bed in a U-shaped microreactor kept in a stream of helium. The gaseous reactants were then carried over the bed by means of this helium stream and into a six-way valve located inside a Varian 3760 gc oven. One loop of the sample valve contained a thermal conductivity detector (intercolumn detector, ICD), which signaled effluent gas flow in the loop, at which time the handle of the six-way valve was moved, injecting the effluent into a Houdry-column system for analysis of gaseous and liquid products. The Houdry system consisted of a 10-ft × $\frac{1}{16}$-in. stainless-steel column filled with microspheroidal Porapak Q and a 27-ft × $\frac{1}{16}$-in. stainless-steel column filled with microspheroidal molecular sieve connected in a T-configuration. The effluent was split to a TCD (three parts), for gas analysis and an FID (one part) for liquid analysis. The oven temperature was kept at 110°C for 9 min after injection via the

TABLE 1

Catalyst Preparations and Properties

Catalyst	Method of Preparation[1]	Calcination Temp. and Time	S.A., m^2/g	Composition[2]
MoO_3	Commercial Product (Fisher) pelleted with stearic acid binder (1%).	500°C, 3.5 hr.	0.8	MoO_3[3]
Bi_2O_3	Commercial Product (Fisher) pelleted with stearic acid binder (1%).	500°C, 3 hr.	0.2	α-Bi_2O_3[4]
$Bi_2O_3 \cdot 3MoO_3$	Coprecipitation from equal volumes of ammonium hydroxide solution of MoO_3 (ammonium molybdate) at pH 6.5 and 10% nitric acid solution of bismuth nitrate.[5]	500°C, 3 hr.	3.1	α-$Bi_2Mo_3O_{12}$[6]
$Bi_2O_3 \cdot 2MoO_3$	Same as $Bi_2O_3 \cdot 3MoO_3$.[7]	500°C, 3 hr.	1.5	β-$Bi_2Mo_2O_9$[8]
$Bi_2O_3 \cdot MoO_3$	Same as $Bi_2O_3 \cdot 3MoO_3$.[9]	500°C, 3 hr.	1.9	γ-Bi_2MoO_6[6]

---

[1] All catalysts ground and screened to 20-35 Mesh size, before calcination.

[2] By x-ray diffraction powder pattern.

[3] Swanson and Fuyat, NBS Circular 539, Vol. III (1953); G. W. Keulks, et. al., Kinet. & Catal., 18,496(1977).

[4] Nat. Bur. Stds. (U.S.) Mono. 25 Sec. 3, 1963.

[5] Bismuth nitrate solution added to stirred molybdate solution, pH adjusted to 3.0, then evaporated at 50°C without filtration.

[6] K. Aykan, J. Catal., 12, 281 (1968); G. W. Keulks, et.al., Kinet. and Catal., 18, 496 (1977).

[7] Bismuth nitrate solution and molybdate solution added simultaneously to same reaction vessel with stirring.

[8] X-ray spectrum similar to that reported [G. W. Keulks, et. al., Kinet and Catal. 18, 496 (1977)], but with a splitting of the 100% peak at 3.19 to a doublet at 3.21 and 3.19 of equal intensity. The spectrum was not consistent with a mixture of the α and β forms.

[9] Molybdate solution added to bismuth nitrate solution with stirring.

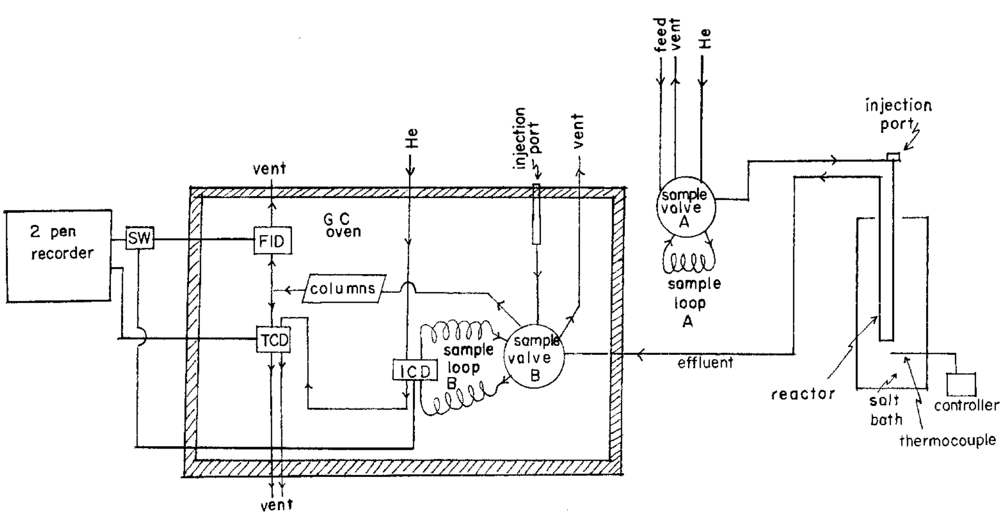

FIG. 1. Pulse microreactor/gc. flow diagram.

six-way valve, then heated to 210°C at a rate of 20°C/min, and kept at 210°C for 15 min. The total He flow through the columns was kept at 20 ml/min (60 psig head pressure) (see Fig. 1).

The six-way valve injector system described above allowed adjustment of reactor flow rate without affecting gc flow rate. For the purpose of comparing runs between different catalysts for a given reactant, the total surface area was kept constant at ~5.4 m^2 by varying the amounts of catalyst used (1.4–3.5 ml). The flow rate was then adjusted to give the same contact time, about 4 sec at 320°C [flow rate (23°C) = 11–26 ml/min].

Yields were determined from absolute response factors (R_f = μmoles/peak area), derived from injections of either a standard gas mixture of known composition (CO_2, propylene, O_2, CO, N_2) via a six-way value (see Fig. 1), or of a known volume (1–10 μl) of a standard solution of acetaldehyde, acrylonitrile, 1,5-hexadiene, 1,3-cyclohexadiene, benzene, and allyl iodide in *n*-octane over fused quartz at 220°C (contact time = 4 sec), conditions under which a negligible amount of decomposition of these compounds occurs. The response factor for acrolein was determined in a similar manner by injection of a freshly distilled sample in aqueous solution. For each component, response factors were determined as a function of the number of μmoles injected (0.01–11 μmoles). The response factor derived from the run closest in peak area to the experimental run in question was used.

As confirmed by control experiments, contact time had little effect on product distribution over MoO_3; consecutive reactions of acrolein and 1,5-hexadiene, and reaction of solvent (*n*-octane) under these conditions was also minimal over MoO_3 at 320°C. Results for other catalysts was corrected for CO_2 formation from solvent.

Prior to each run, the catalyst was heated at 430°C under a stream of air for 20 min., then placed under Helium stream for 10 min. The pulses of sample were then introduced as described above by microsyringe.

RESULTS AND DISCUSSION

(*A*) *Thermal Decompositions*

1. Azopropene (**1**). As reported previously (*4*), the thermal decomposition of azopropene gave quantitative yields of N_2 and 1,5-hexadiene, the product of dimer-

TABLE 2

Thermal Decomposition of Allyl Iodide and Azopropene at 320°C over Fused Quartz

Exp.	Reactant	μ moles used	Contact time	% yields				
				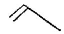	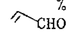	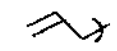		N_2
1		9.9	3.6 sec.	0.3 (0.3)	0.1 (0.1)	32.4 (30.7)	72.7 (68.9)	-
2	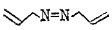	6.3	3.6 sec.	0.8 (0.8)	-	102 (99.2)	-	97.7 (100)

Numbers in ( ) are normalized to 100% total carbon balance.

ization of two allyl radicals (see Table 2, Expt 2).

2. Allyl iodide. Under conditions the same as for the decomposition of 1, allyl iodide gave 1,5-hexadiene (31% yield) as the major product, along with a trace of propylene, the balance being unreacted allyl iodide (69%) (see Table 2, Expt. 1). The thermal reaction, then, appears to be a homolytic C–I cleavage, followed by recombination. The lower conversion when compared to azopropene reflects the higher activation energy (43.5 vs 36.1 kcal/mole, respectively).

(*B*) MoO_3

1. Effect of concentration. The results over MoO_3, as with the other catalysts studied, were found to exhibit a trend toward greater interaction of allyl iodide, azopropene, and allyl radicals on dilution, reflected in smaller 1,5-hexadiene (the product of thermal dimerization of two allyl radicals) yields and larger oxidation product yields (see Table 3). This is probably the result of a more homogeneous distribution of reactant molecules over the catalyst surface, increasing the likelihood of reaction with catalyst over dimerization.

2. Propylene. Reaction of propylene with MoO_3 at 320°C, 4 sec contact time, gave 100% propylene breakthrough, in good agreement with Haber's results (*3a*) (see Table 4, Expt. 1). Since there are no α-hydrogen abstracting sites, no reaction can occur.

3. Allyl iodide. In agreement with Haber's work (*3a*), the major product is acrolein, the absolute yield of which increases on dilution (see Table 3, Expts. 1 and 2). Since almost no dimerized products are formed under these dilute conditions, gas phase reactions are minimal. The lower material balance for the neat samples is indicative of carbonaceous deposition, resulting from inhomogeneous distribution of allylic species, dimerization and polymerization occurring on areas of the catalyst in which a high concentration of allylic species are present. As expected, the yield of acrolein dropped sharply with pulse number, and that of 1,5-hexadiene and benzene rose, the total conversion falling to 79% (see Table 5, Expts. 1 and 2).

4. 1,5-Hexadiene. As can be seen from Table 6, Expts. 1 and 2, 1,5-hexadiene undergoes only minor decomposition at 320°C over MoO_3, 4 sec contact time (98.4 and 91.4% breakthrough for the neat and 0.036 *M* solution in *n*-octane, respectively). Under these conditions, 10 μl of *n*-octane undergoes no detectable oxidation over MoO_3. This data (Table 6, Expt. 2) will be used to determine the contribution of the gas phase thermal reaction in the azopropene experiments described below.

5. Azopropene. Under neat conditions, where 81% carbon and 84% nitrogen balances are obtained, the major product is 1,5-hexadiene (see Table 3, Expts. 3–6). However, as one decreases the amount of sample, and, more drastically, by dilution, much lower nitrogen (44%) and carbon (37%) balances are obtained. At the same time, higher yields of acrolein, benzene, acetaldehyde, propylene, and CO_2 are found, at the expense of the 1,5-hexadiene yield. These results are again interpreted in terms of a greater interaction of allyl radicals and azo compound with catalyst. This latter effect results in competition between thermal decomposition, which yields N_2 (84% in neat samples) and chemisorption of azo compound, which may result in isomerization of **1** to hydrazone **2**, which could undergo N–N cleavage and further oxidation to give the observed acrylonitrile (AN) (see Scheme 1). Alternatively, the hydrazone **2** could remain chemisorbed, or desorb; under the analysis conditions **2** would not be detected. In any event chemisorption of azo compound **1** will probably lead to lowered N_2 yields.

SCHEME 1. Formation of **2** and AN from **1** and MoO_3.

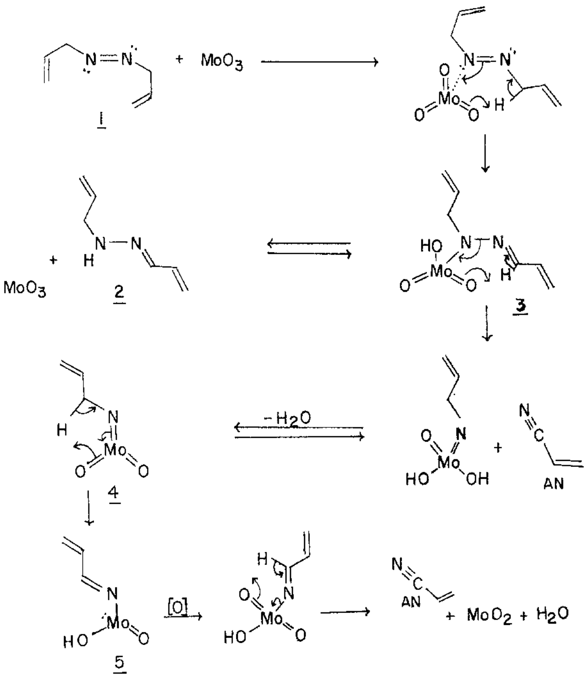

A probable mechanism for the reaction of azopropene with MoO_3 to give *N*-allyl acrolein hydrazone (**2**) and acrylonitrile (AN) is outlined in Scheme 1. Initial chemisorption of the azo compound on MoO_3 via the lone pairs in nitrogen, followed by an "ene" reaction, gives intermediate **3**, which can either give **2** after elimination of MoO_3 with proton transfer, or form AN and the molybdenum VI imine **4** via a 1,5-hydrogen transfer, followed by dehydration. Intermediate **4**, after undergoing a 1,4-hydrogen transfer, forms the molybdenum IV species **5**, which can give MoO_2 plus another molecule of AN after oxidation and subsequent 1,4-hydrogen transfer.

Lowering the reaction temperature to 238°C gives only a 25% yield of N_2, and only an 8% C balance consistent with a

TABLE 3

Effect of Concentration on Product Yield at 320°C over MoO_3(1)

Exp.	Reactant	μ moles, Conditions	CO/CO_2	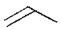	CH_3CHO	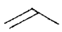CHO	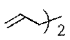	ØH		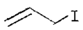	N_2	AN	% C. bal.
1	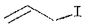	9.9, neat	-/0.3	0.8	0.5	76.4	1.0	2.4	-	1.0	-	-	82.4
			(-/0.4)	(1.0)	(0.6)	(92.7)	(1.2)	(2.9)	-	(1.2)			
2	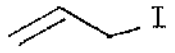	0.75 (10 μl of 0.75M	1.6/5.6	12.0	1.3	84.9	-	0.3	-	-	-	-	105.7
		in n-octane)^2	(1.5/5.3)	(11.4)	(1.2)	(80.3)	-	(0.3)	-	-	-	-	
3	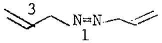 1	9.7, neat	0.4/1.5	1.0	3.1	2.0	71.3	0.4	1.0	-	84.3	-	80.7
			(0.5/1.9)	(1.2)	(3.8)	(2.5)	(88.4)	(0.5)	(1.2)				
4	"	6.7, neat	0.5/1.9	1.0	4.4	2.6	61.4	0.4	1.7	-	78.7	1.9	75.8
			(0.6/2.5)	(1.3)	(5.8)	(3.4)	(81.0)	(0.5)	(2.2)			(2.5)	
5	"	4.9, neat	-/0.9	0.9	2.3	3.2	45.7	0.4	0.3	-	61.9	2.0	55.8
			(-/1.6)	(1.6)	(4.1)	(5.7)	(82.0)	(0.7)	(0.5)			(3.6)	
6	"	0.6-0.8 (10 μL of 0.06-0.08M in n-octane) avg. of 4 runs	-/4.0	1.8	3.5	11.6	10.2	2.6	-	-	44.0	3.4	37.1
			(-/10.8	(4.9)	(9.4)	(31.3)	(27.5)	(7.0)				(9.2)	
7	"	6.2, neat, 238°C	-	2.4	0.3	1.3	3.5	0.06	-	-	24.8	0.6	8.2

(1) Contact time = 4 sec., total surface area = $5.3m^2$, numbers in ( ) are normalized to 100% total carbon balance.

(2) Average of 3 runs

TABLE 4

Reaction of Propylene over Bi/Mo-Containing Catalysts at 320°C

Exp.	Catalyst	Contact Time	Surface Area, tot.	μ moles 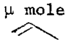	CO/CO$_2$	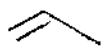	CH$_3$CHO	CHO	2	ØH	Selectivity to CHO	% C bal.
1	MoO_3	4.0 sec.	5.6 m^2	11.2	-	102 (100)	-	-	-	-	-	102 (100)
2	$Bi_2O_3 \cdot 3MoO_3$	4.4 sec.	6.1 m^2	11.2	-/0.3 (0.3)	88.4 (92.5)	0.3 (0.3)	6.5 (6.8)	-	0.1 (0.1)	90.3	95.6 (100)
3	$Bi_2O_3 \cdot 2MoO_3$	4.0 sec.	5.8 m^2	11.4	-/0.3 (0.3)	90.8 (93.5)	-	5.7 (5.9)	-	0.3 (0.3)	90.5	97.1 (100)
4	$Bi_2O_3 \cdot MoO_3$	4.2 sec.	5.9 m^2	10.9	-/0.1 (0.1)	96.5 (98.6)	-	0.7 (0.7)	-	0.6 (0.6)	50	97.9 (100)
5	Bi_2O_3	4.0 sec.	2.9 m^2	11.1	-/0.3 (0.3)	101 (99.5)	-	-	0.2 (0.2)	-	-	101.5 (100)
6	$M_a^{2+}M_b^{3+}Bi_xMo_yO_z$ (See Ref. 8)	4.4 sec.	6.1 m^2	10.3	0.8/1.6 (0.8)/(1.7)	28.1 (29.7)	0.04 (0.04)	63.6 (67.2)	-	0.5 (0.5)	95.7	94.6 (100)

Numbers in ( ) are normalized to 100% total carbon balance.

TABLE 5

Effect of Pulse Number of Yields over MoO_3 at 320°C[1]

Exp.	Pulse #	Reactant	μ moles, Conditions	CO/CO_2	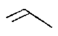	CH_3CHO	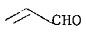	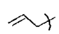 2	ØH		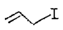	N_2	AN	C Bal
1	1	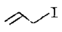	9.9, neat	-/0.3 (0.4)	0.8 (1.0)	0.5 (0.6)	76.4 (92.7)	1.0 (1.2)	2.4 (2.9)	-	1.0 (1.2)	-	-	82.4 (100)
2	2	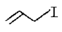	9.4, neat	-/0.1 (0.1)	1.3 (1.6)	-	43.9 (54.9)	8.0 (10.0)	5.6 (7.0)	-	21.0 (26.3)	-	-	79.9 (100)
3	1	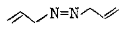	4.8, neat	-/0.9 (1.6)	0.9 (1.6)	2.3 (4.1)	3.2 (5.7)	45.7 (82.0)	0.4 (0.7)	0.3 (0.5)	-	61.9	2.0 (3.6)	55.7 (100)
4	2	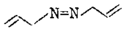	5.6, neat	0.2/0.5 (0.3/0.7)	0.5 (0.7)	1.8 (2.5)	2.2 (3.0)	64.8 (89.6)	0.1 (0.1)	0.2 (0.3)	-	70.4	2.0 (2.8)	72.3

[1] 4 sec. contact time, $5.3m^2$ total surface area; numbers in ( ) are normalized to 100% total carbon balance.

TABLE 6

Catalytic Reactions of 1,5-Hexadiene at 320°C[1]

Exp.	Catalyst	Surface Area Used	Contact Time	μ moles			% yields					%
				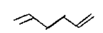	CO/CO_2	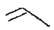	CH_3CHO (normalized)	 CHO	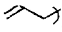	ØH		C bal.
1	MoO_3	5.3m^2	3.9 sec.	6.3, neat	-/0.7 (0.8)	-	0.5 (0.6)	0.08 (0.1)	82.2 (98.4)	trace	-	83.5 (100)
2	MoO_3	5.3m^2	4.2 sec.	0.36, 10μL of 0.036M in n-octane	-/6.6 -(6.3)	trace	1.5 (1.4)	0.3 (0.3)	95.9 (91.4)	0.3 (0.3)	0.3 (0.3)	104.9 (100)
3	$Bi_2O_3 \cdot 3MoO_3$	5.6m^2	3.9 sec.	6.7, neat	-/0.2 (0.6)	0.3 (1.0)	0.3 (1.0)	trace	16.9 (55.8)	4.4 (14.5)	8.2 (27.1)	30.3 (100)
4	$Bi_2O_3 \cdot 2MoO_3$	5.5m^2	3.8 sec.	6.3, neat	-/0.3 (0.7)	-	0.2 (0.5)	trace	19.0 (42.6)	13.7 (30.7)	11.4 (25.6)	44.6 (100)
5	$Bi_2O_3 \cdot MoO_3$	5.4m^2	3.8 sec.	6.3, neat	-/0.4 (0.8)	-	-	-	17.3 (36.0)	19.1 (39.7)	11.3 (23.5)	48.1 (100)
6	Bi_2O_3	2.7m^2	3.8 sec.	5.9, neat	-/2.9 (2.7)	-	-	-	101 (94.7)	-	2.7 (2.5)	106.6 (100)

---

[1] Numbers in ( ) are normalized to 100% total carbon balance.

strong chemisorption of azo compound (see Table 3, Expt. 7). As expected, the yields of oxidized products fall, due to loss of lattice oxygen, while that of 1,5-hexadiene and the overall carbon and nitrogen balances increase with the second pulse of azopropene probably due to partial blocking of azo chemisorption site (see Table 5, Expts. 3 and 4).

Thus, the product distributions shown in Table 3 for azopropene 1 represent a composite of gas phase dimerization and reaction with MoO_3 of allyl radicals (7). If one assumes that all the 1,5-hexadiene formed resulted from gas phase dimerization of allyl radicals, by subtracting the yields of products from the 1,5-hexadiene reaction over MoO_3 (which gives mainly unreacted 1,5-hexadiene (see Table 6, Expts. 1 and 2), the corrected yields for the interaction of allyl radicals with MoO_3 can be obtained. The results of these calculations are recorded in Table 7.

From Table 7 it can be seen that the ratio of gas phase dimerization of allyl radicals to reaction with MoO_3 for dilute samples has been reduced to 25.6:51.1 or about 1:2 from the 9:1 (calculated from a similar analysis of the data in Expt. 3, Table 3) found for the neat samples. The data in Table 7 is depicted graphically in Scheme 2 along with the analogous allyl iodide reaction.

SCHEME 2. Azopropene and allyl iodide reactions over MoO_3 at 320°C.

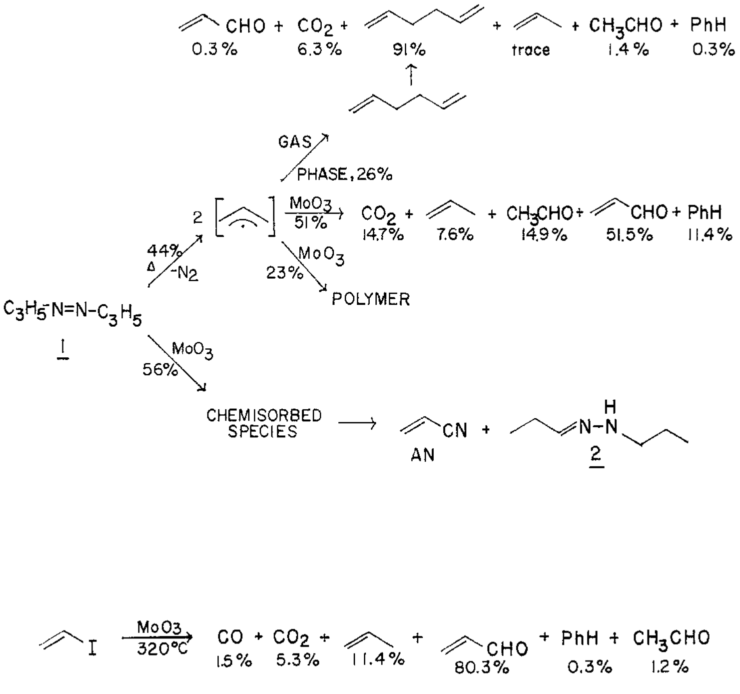

Under these dilute conditions, allyl radicals give a much larger percentage of acetaldehyde, CO_2, and benzene, and less acrolein than does allyl iodide under the same conditions (compare lines 5 and 7 of Table 7). This is highly suggestive that free allyl radicals are not the intermediate in the major pathway leading from allyl iodide plus MoO_3 to acrolein at 320°C.

This formation of benzene from the interaction of allyl radicals with MoO_3 deserves comment (see Table 7, line 4). Since

TABLE 7

Comparison of Yields for Allyl Radicals and Allyl Iodide with MoO_3 at 320°C, 4 sec

Line No.	Reactant	Significance of % yields	CO/CO_2	N_2	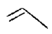	CH_3CHO	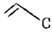CHO	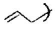2	ØH	C bal.
1	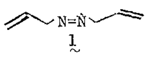	% yield[1]	-/4.0	44	1.8	3.5	11.6	10.2	2.6	33.7
2		Normalized wrt. 100% N_2 Yield (100% allyl radicals)	-/9.1	100	4.1	8.0	26.4	23.2	5.9	76.7
3		From gasphase reaction[2] (1,5 hexadiene + MoO_3)	-/1.6	-	0.2	0.4	0.1	23.2	0.1	25.6
4		From MoO_3 + allyl radical[3]	-/7.5	100	3.9	7.6	26.3	0	5.8	51.1
5		Normalized, MoO_3 + allyl radical[4]	-/14.7	100	7.6	14.9	51.5	0	11.4	100
6	 I	% yield	1.6/5.6	-	12.0	1.3	84.9	-	0.3	105.7
7		Normalized % yield[5]	1.5/5.3	-	11.4	1.2	80.3	-	0.3	100

[1] Table III, exp. 6

[2] Table VI, exp. 2, normalized to 23.2% 1,5-hexadiene

[3] Subtract line 3 from line 2

[4] Line 3 normalized to 100% carbon balance

[5] From Table III, exp. 2

only about 0.3% benzene (Table 7, Expt. 2) is formed from the reaction of 1,5-hexadiene over MoO_3 under the conditions of the azopropene experiment, the formation of benzene from allyl radicals + MoO_3 (11.4%, see Table 7, line 5) must result from dimerization of two chemisorbed allyl radicals, which form a chemisorbed C_6 derivative not accessible via reaction of 1,5-hexadiene with MoO_3. This C_6 species is then dehydrogenated, cyclizes, and again dehydrogenates to form benzene.

These results show that free allyl radicals are much more waste forming than is allyl iodide in the reaction with MoO_3 at 320°C, and suggests that allyl radicals, while they may form acrolein via the allylic intermediate of propylene oxidation, are not themselves the selective intermediate in catalytic oxidation of propylene.

The formation of acrolein from allyl radicals over MoO_3 is shown in Scheme 3.

SCHEME 3. Formation of acrolein and AN from 1 + MoO_3.

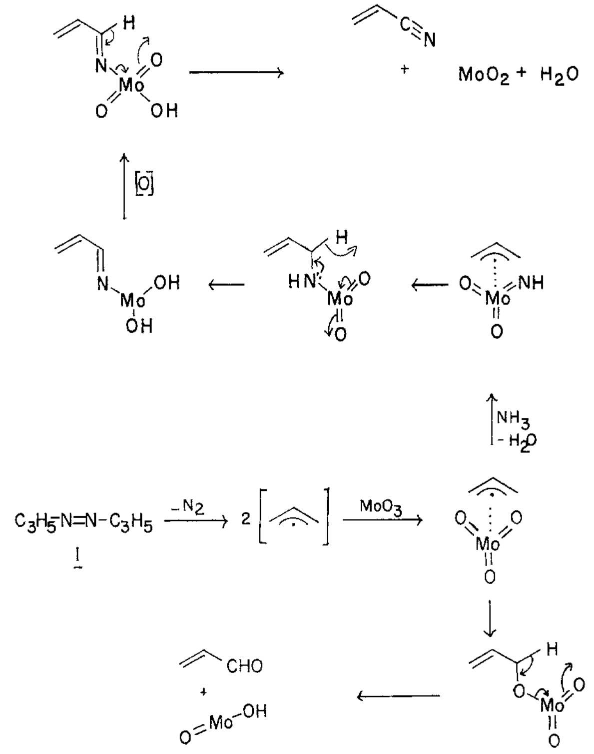

Initial chemisorption, collapse to form the Mo(V) ester, and subsequent H abstraction is depicted.

(C) $Bi_2O_3 \cdot 3MoO_3$, $Bi_2O_3 \cdot 2MoO_3$

1. Propylene. Under the same conditions used in the MoO_3 experiments, $Bi_2O_3 \cdot 3MoO_3$ and $Bi_2O_3 \cdot 2MoO_3$ used in these experiments (see Table 1) are very similar in selectivity, ~90%, and activity, ~12% and 9% conversion, respectively (see Table 4, Expts. 2 and 3).

2. Allyl iodide. Reactions of neat allyl iodide gave very poor material balances over these catalysts (~40%), while 92–98% (2 sec) balances were obtained from dilute solutions. (Table 8, Expts. 1–7). This is probably due to generation of high concen-

TABLE 8

Reaction of Allyl Iodide over $Bi_2O_3 \cdot nMoO_3$ at 320°C

Exp.	n	µ moles  I	S.A. m^2	Conditions	Contact time	CO/CO_2[1]	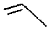	CH_3CHO	%yields  CHO (Normalized)	 2	ØH		 I	C bal.
1	3	10.8	6.1	neat (ave. 2 runs)	3.9	-/0.8	11.0	1.4	19.1	-	1.4	-	0.5	34.2
2	3	10.5	"	neat, pulse #2	3.9	-/0.4	15.5	0.7	5.5	-	1.2	0.5	0.1	23.9
3	3	0.33	"	4.3µL of 0.077M in n-octane	2	-/0 (-/0)	1.6 (1.7)	4.8 (5.2)	76.8 (83.8)	-	8.8 (9.6)	-	-	92.0 (100)
4	3	0.33	"	"	1	-/0 (-/0)	1.2 (1.3)	1.9 (2.1)	80.0 (87.2)	- -	6.0 (6.5)	- -	2.6 (2.8)	91.7 (100)
5	2	9.9	5.8	neat	3.8	-/1.0	11.5	1.5	10.8	0.4	1.6	0.3	-	27.1
6	2	10.5	"	neat, pulse #2	3.8	-/0.2	15.9	0.4	5.8	9.1	3.2	2.8	-	37.4
7	2	0.33	"	4.3µL of 0.077M in n-octane	2	-/1.2 (-/1.3)	8.7 (9.2)	1.1 (1.2)	75.5 (80.2)	3.5 (3.8)	4.1 (4.4)	-	-	94.1 (100)
8	2	"	"	"	1	-/0.5 (-/0.7)	4.3 (5.9)	trace	64.0 (88.2)	1.8 (2.5)	1.9 (2.6)	-	-	72.5 (100)
9	1	10.2	5.9	neat, (ave. 2 runs)	3.8	-/2.0	14.3	0.8	2.1	0.8	5.6	0.6	-	26.2
10	1	10.8	"	neat, pulse #2	3.8	-/1.0	13.8	0.9	2.9	6.1	6.2	2.9	-	33.8
11	1	0.33	"	10µL of 0.033M in n-octane	2	-/3.6	8.2	-	4.8	0.7	1.8	-	-	19.1
12	0	9.3	2.7	neat	3.8	-/4.8	1.2	-	-	50.1	-	0.8	6.6	63.5
13	0	9.9	"	neat, pulse #2	3.8	-/2.0	0.9	-	-	70.8	-	1.8	3.2	78.7

---

[1] Corrected for formation of CO/CO_2 from n-octane where appropriate.

trations of allylic species on the surface, for the neat samples, resulting in dimerization and/or polymerization. Poor material balances were also obtained for 1,5-hexadiene over these catalysts (Table 6, Expts. 3 and 4), and thus dimer, once formed, would be strongly chemisorbed. The deposition of carbonaceous material was confirmed by pulsing the catalyst with O_2 at 430°C after reaction of neat samples, which resulted in large amounts of CO_2 formation.

3. Azopropene. Reaction of azopropene over these catalysts, both neat and diluted in *n*-octane (for $Bi_2O_3 \cdot 3MoO_3$), gave very poor material balances (Table 9, Expts. 1–6). As with allyl iodide, this is probably due to dimerization of the allyl radicals, since interaction of 1,5-hexadiene with these catalysts gave a similar product distribution and carbon balance (Table 6, Expts. 3 and 4). To a lesser extent, chemisorption/isomerization of azo compound is involved, since nitrogen balances are 60 to 90%. These experiments generate allylic fragments (radicals) probably in much closer proximity than they are produced from propylene, resulting in predominantly dimer (and/or polymer) formation, with only small amounts of oxygen insertion products. Very drastic increases in 1,5-hexadiene and carbon balances, and lesser increases in N_2 and benzene, occur with increasing pulse number, again consistent with a partial blocking of the 1,5-hexadiene and azo chemisorption sites. Product distribution changes indicative of greater interaction of azo compound and allyl radicals with catalyst occur on dilution of azopropene in *n*-octane.

(*D*) $Bi_2O_3 \cdot MoO_3$, Bi_2O_3

1. Propylene. Both of these catalysts are very inactive at 320°C, giving only traces of CO_2, acrolein, and benzene at 97% breakthrough for $Bi_2O_3 \cdot MoO_2$ and traces of CO_2 and 1,5-hexadiene at about 100% breakthrough for Bi_2O_3 (see Table 4, Expts. 4 and 5). The low activity of Bi_2O_3 shows that, if it is strictly bismuth polyhedra that are associated with α-hydrogen abstraction, then some other process, which is part of the rate-determining step, must also be facilitated for reaction to occur, probably chemisorption of propylene on Mo.

2. Allyl iodide. Very low (19–34%) material balances were obtained in both neat and dilute systems, small amounts of propylene and acrolein being the main products (see Table 8, Expts. 9–13). Polymerization of allylic fragments is the probable source of low material balance over these catalysts low in oxygen insertion capabilities.

3. Azopropene. Low (~15%) carbon balances for $Bi_2O_3 \cdot MoO_3$ is due to chemisorption of azo (N_2 yield ~65%) and dimerization of allyl radicals (Table 9, Expts. 7 and 8), since 1,5-hexadiene also gives low carbon balances when injected over this catalyst under the same conditions (Table 6, Expt. 5). The main products are 1,5-hexadiene (~2%), benzene (~3%), and propylene (5.6%) (see Table 9, Expts. 7 and 8).

Somewhat higher carbon balances (~63%) are obtained for Bi_2O_3 (Table 9, Expts. 9 and 10), reflecting the nearly quantitative breakthrough of 1,5-hexadiene under these conditions (Table 6, Expt. 6). Nitrogen yields are higher (~73%) than for $Bi_2O_3 \cdot MoO_3$, due to less affinity for chemisorption/isomerization. As in the propylene and allyl iodide reactions, the low ability of Bi_2O_3 to insert oxygen is reflected in the product distribution.

(*E*) *Propylene Oxidation over Multicomponent Catalyst* ($M_a^{2+}M_b^{3+}Bi_xMo_yO_z$) (*8*) *320°C*

When compared to $Bi_2O_3 \cdot 3MoO_3$, $Bi_2O_3 \cdot 2MoO_3$, and $Bi_2O_3 \cdot MoO_3$, the multicomponent catalyst is much more active (70% conversion) and selective (95% to acrolein)

TABLE 9

Reaction of Azopropene over $Bi_2O \cdot nMoO_3$ at 320°C

Exp.	n	μ mole 1	Conditions	Contact Time, sec.	S.A. m^2	CO/CO_2[1]	% yields 	CH_3CHO	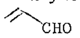	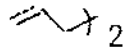	ØH		N_2	AN	C bal.
1	3	10.1	neat	3.9	6.1	0.1/1.4	3.0	1.7	0.1	13.7	1.6	4.1	71.7	1.9	27.6
2	3	6.3	neat	3.9	"	0.4/1.8	2.3	2.1	0.1	3.6	2.8	3.0	87.5	1.9	18.0
3	3	6.3	neat, pulse #2	3.9	"	0.2/1.6	1.5	2.2	0.1	36.6	2.1	10.4	90.3	1.9	56.6
4	3	0.25	10μL of 0.025M in n-octane	~2	"	-/-	1.7	2.9	11.5	0.6	0.8	-	58	9.1	26.6
5	2	6.2	neat	3.8	5.8	-/0.3	2.7	0.7	0.2	4.2	6.9	3.3	70.3	1.6	19.9
6	2	5.6	neat, pulse #2	3.8	"	-/0.2	2.1	1.0	0.2	26.1	6.8	7.5	82.4	2.0	45.9
7	1	5.7	neat	3.8	5.9	-/0.7	5.6	-	-	2.1	3.5	1.2	53.7	1.8	14.9
8	1	5.7	neat, pulse #2	3.8	"	-/0.7	4.5	-	-	15.5	5.7	8.5	66.0	1.9	36.8
9	0	4.8	neat	3.8	2.7	-/2.7	1.0	-	-	54.9	0.2	1.6	73.1	2.2	62.6
10	0	5.2	neat, pulse #2	3.8	2.7	-/trace	1.0	-	-	63.7	-	3.2	75.9	1.4	69.3

---

[1] Corrected for formation of CO/CO_2 from n-octane, where appropriate.

under the same conditions (see Table 4, Expt. 6). The higher activity and selectivity of the multicomponent system suggests more effective catalytic sites are operative in the multicomponent system. While Bi and Mo are still involved as the prime site where chemisorption of propylene, α-H abstraction, and oxygen (or NH) insertion occur, the added components of the catalyst facilitate the reconstruction of the active site via facilitated oxygen transfer to the active Bi–O–Mo site and by altering the structural and electronic environment of these primary sites. Shear structures and solid solutions of the multicomponent system are responsible for this higher efficiency in conjunction with facilitated electron exchange achieved by the multiplicity of near lying and readily exchangeable electronic states of the catalysts' multicomponent nature.

(*F*) *Ammoxidation Mechanistic Studies*

It is a well-known phenomenon that, while oxidation of propylene to acrolein over Bi/Mo catalysts occurs readily at 320°C, upon addition of ammonia to the feed, no propylene conversion occurs until about 400°C. We believe that blocking of propylene chemisorption sites by ammonia at 320°C may be responsible for this phenomenon. Only at higher temperatures is ammonia reversibly activated, allowing propylene to be activated on an empty site, and then interacting with the activated propylene. If this is true, and if allyl radicals can generate the active allylic intermediate over MoO_3, then generation of allyl radicals over MoO_3 at 320°C in the presence of ammonia should effectively by-pass the rate-determining step of propylene activation (chemisorption, α-hydrogen abstraction) and allow AN formation to occur. In fact, when NH_3 and allyl radicals, generated from azopropene, are allowed to react over MoO_3 at 320°C, about 6% more AN is formed (at the expense of acrolein) than when no ammonia is present (see Table 10, Expts. 1 and 2). In these two experiments, the total AN + acrolein is about the same. However, if MoO_3 is prereduced with about the same number of μmoles NH_3 as in the competitive experiment, and then pulsed with allyl radicals (from azopropene), only a trace of acrolein is formed and about 1% more AN than in the reaction with no NH_3 over oxidized MoO_3 (Table 10, Expt. 3). The major product is 1,5-hexadiene, about twice as much as with no ammonia over oxidized MoO_3. These experiments are consistent with a mechanism in which allyl radicals compete favorably with ammonia for oxygen insertion sites. When no allyl radicals are present, ammonia blocks propylene chemisorption sites; when the catalyst is subsequently pulsed with allyl radicals, only a trace of acrolein is formed, and the AN formed results from isomerization and cleavage of the azo compound (see Scheme 1).

Since the reaction of acrolein and ammonia with MoO_3 under these conditions does give mainly AN (51.6%, see Table 10, Expt. 4), it is possible that AN, in these experiments, could result from further reaction of initially formed acrolein, or from direct insertion of nitrogen into the allyl radical. In either case, our conclusions concerning the competition of allyl radicals and ammonia for oxygen insertion sites are still valid.

A probable mechanism for formation of AN from allyl radicals, MoO_3, and ammonia is shown in Scheme 3.

CONCLUSIONS

From the difference in product distribution between the reaction of allyl iodide and allyl radicals (from azopropene) over MoO_3 at 320°C, it can be seen that the former reaction does not involve the initial formation of allyl radicals which then interact with catalyst. While acrolein is the

TABLE 10

Reaction of Azopropene with MoO_3 at 320°C in the Presence of Excess NH_3[a]

Exp.	μ moles 1	μ moles NH_3	Conditions	Contact time, sec	CO/CO_2	N_2	% yields 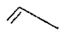	CH_3CHO	 CHO		ØH	AN	C bal
1	0.43	16.5	10μL of 0.043M in n-octane + 1.1μL 15M NH_3 in H_2O	4.2	–/5.5	104[b]	3.7	-	4.2	11.3	1.9	8.8	35.4
2	0.43	0	10μL of 0.043M in n-octane	4.2	-/6.1	50.3	1.8	1.2	9.4	14.1	2.6	3.2	38.4
3	0.43	0	10μL of 0.043M in n-octane, after pretreatment with 11μ mole NH_3	4.2	-/5.9	58.5	1.5	-	0.6	27.1	3.3	4.1	42.5
4	0	13	0.28μ mole  CHO (10μL of 0.028M in n-octane + 0.9μL of 15M NH_3 in H_2O)	4.2	-/15.6	-	-	-	19.1	2.0	8.6	51.6	96.9

---

[a] Total surface area = 5.6m^2.

[b] High due to oxidation of NH_3.

major product of allyl radicals over MoO_3 at 320°C (52%, Table 7, line 5), the larger amounts of CO_2, acetaldehyde, and benzene formed, compared with the allyl iodide experiment (see Table 7, compare lines 5 and 7), or propylene over bismuth molybdates (see Table 4, Expts. 2–4 and 6), suggest that allyl radicals may, in part, form, but are not themselves the selective intermediate in catalytic propylene oxidation.

The formation of propylene from allyl iodide (2 electron reduction) and allyl radicals (1 electron reduction) over the catalysts studied (Tables 3, 8, and 9) probably occurs on reduced catalyst sites, in which hydrogen atoms are donated from surface hydroxyl groups, resulting in oxidation of these sites.

The data for the oxidation of allyl iodide (Table 8), azopropene (Table 9), and propylene (Table 4) over $Bi_2O_3 \cdot nMoO_3$ show that, for both $n = 3$ and $n = 2$, similar activities and selectivities are found, while for $n = 1$, these values are much less. This is consistent with the theory that for $n = 1$, there are mostly regeneration sites, while for $n = 2$ and $n = 3$, both oxygen insertion and regeneration sites are present. This is also consistent with the relative reoxidation rates

$$(Bi_2O_3 \cdot 3MoO_3 \approx Bi_2O_3 \cdot 2MoO_3 \ll Bi_2O_3 \cdot MoO_3),$$

which will be presented in more detail in a forthcoming paper.

Thus, the data are consistent with a mechanism involving a concerted chemisorption of propylene on the active site **6** (probably on molybdenum centers) α-hydrogen abstraction (by bismuth oxygens) to form **7** in the rate-determining step, followed by fast oxygen (or NH) insertion (molybdenum oxygens) to form **8** (or **10**) and subsequently acrolein, or AN if ammonia is present (see Scheme 4). This

SCHEME 4. Proposed mechanism for oxidation and ammoxidation of propylene.

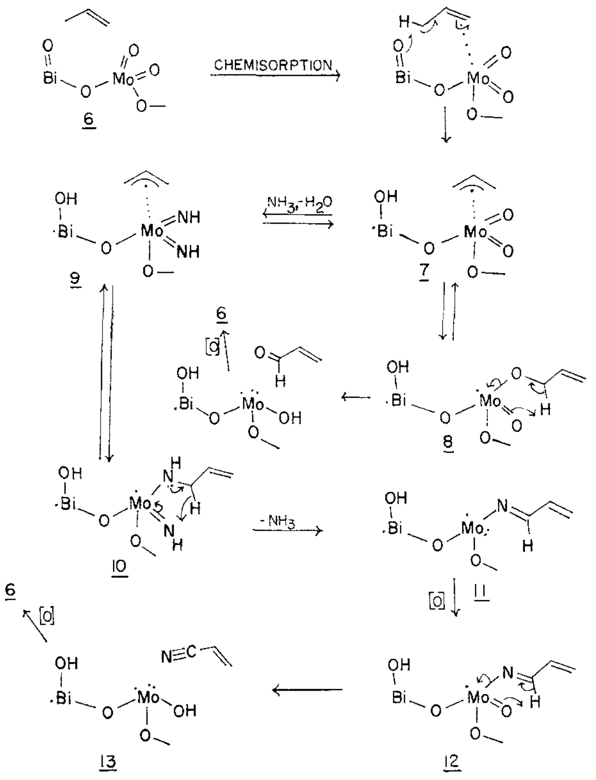

would explain the fact that very little or no reaction of propylene occurs over Bi_2O_3 or MoO_3 at 320°C, since the former lacks the chemisorption, and the latter the hydrogen abstracting ability, required by the rate-determining step.

The proposed mechanism in Scheme 4 is also consistent with the observed kinetics (first order in propylene) (*1a, b*) and deuterium isotope effects (*2g, 9*). A significant fact concerning ammoxidation of propylene over U/Sb catalyst is that when 1-d_2 propylene is ammoxidized, the ratio of CH_2CHCN to CD_2CHCN (1.5:1) is that expected on the basis of a deuterium isotope effect in the removal of hydrogen or deuterium from (CD_2CHCH_2). In order to account for this, there must be a rapid equilibrium between molybdenum (V) amide **10** and the allylic complex **9** (see Scheme 4).

The presence of metal–oxygen double bonds is an important feature of the proposed mechanism (Scheme 4). The importance of such bonds in selective oxidation catalysts has been recognized by Trifiro *et al.* (*10*). In this mechanism, the bismuth–oxygen double bonds are responsible for α-hydrogen abstraction to form **7** while those of molybdenum are responsible for oxygen insertion to form **8**, hydrogen abstraction from the σ-allylic intermediate **8** to form acrolein, formation of the NH species **9** by reaction with ammonia, and the subsequent H-abstractions leading to AN (**10** → **11**, **12** → **13**).

We have, then, in this work presented good evidence that free allyl radicals are probably not the *selective* intermediate in propylene oxidation, but have also shown that these allyl radicals can be converted to acrolein with about 50% selectivity over MoO_3 at 320°C (Table 7). Assuming this, 50% of the free allyl radicals form an intermediate similar to that formed after the chemisorption, α-hydrogen abstraction step in the oxidation of propylene over bismuth molybdate (7). The formation of AN from interaction of allyl radicals with MoO_3 at 320°C in the presence of excess ammonia is consistent with the theory that ammonia deactivates propylene oxidation at this temperature by supression of the rate-determining step, which forms the allylic intermediate **7**. However, once this intermediate is formed, it can produce AN in the presence of ammonia at 320°C.

REFERENCES

1. (*a*) Hucknall, D. J., "Selective Oxidation of Hydrocarbons," p. 24. Academic Press, New York, 1977, and references cited therein. (*b*) Callahan, J. L., Grasselli, R. K., Milberger, E. C., and Strecker, H. A., *I & EC Prod. Res. & Dev.* **9**, 134 (1970); (*c*) Godin, G. W., McCain, C. C., and Porter, E. A., *Proc. Fourth Int. Cong. Cat., Moscow*, 1968, paper 20; (*d*) Sachtler, Wm. H., *Rec. Trav. Chim.* **82**, 243 (1963).
2. (*a*) Haber, J., and Grzybowska, B., *J. Catal.* **28**, 489 (1973); (*b*) Hart, P. J., and Friedli, H. R., *Chem. Commun.* 621 (1970); (*c*) Weiss, F., Marion, J., Metzger, J., and Cognion, J. M., *Kinet. Catal.* **14**, 32 (1973); (*d*) Peacock, J. M., Parker, A. J., Ashmore, P. G., and Hockey, J. A., *J. Catal.* **15**, 398 (1969); (*e*) **15**, 379 (1969); (*f*) Adams, C. R., *Proc. Int. Congr. Catal.* **1**, 240 (1965); (*g*) Adams, C. R., and Jennings, T. J., *J. Catal.* **3**, 549 (1964); **2**, 63 (1963).
3. (*a*) Grzybowska, B., Haber, J., and Janas, J., *J. Catal.* **49**, 150 (1977); (*b*) Sokolouskii, V. D., and Bulgakov, N. N., *React. Kinet. Catal. Lett.* **6**, 65 (1977); (*c*) Zhiznevskii, V. M., Vanyk, L. I. I., and Yakubovskaya, O. F., *Russian J. Phys. Chem.* **51**, 902 (1977).
4. Al-Sader, B. H., and Crawford, R. J., *Canad. J. Chem.* **48**, 2745 (1970).
5. Sibbett, D. J., and Noyes, R. M., *J. Amer. Chem. Soc.* **75**, 761 (1953).
6. Azopropene purified by this method gave NMR ($CDCl_3$) consistent with the structure: 4.40δ (d, 4H), 5.17δ (br s, 2H), 5.32δ (d, 2H), 5.9–6.3δ (m, 2H).
7. AN probably results from the chemisorption scheme discussed above and depicted in Scheme 1.

8. Grasselli, R. K., and Hardman, H. F., U. S. Patent 3,642,930 (15 Feb. 1972); Grasselli, R. K., Miller, A. F., and Hardman, H. F., Ger. Offen. 2,147,480 (4 May 1972); Grasselli, R. K., Miller, A. F., and Hardman, H. F., Ger. Offen. 2,203,709 (17 Aug. 1972).

9. Grasselli, R. K., and Suresh, Dev. D., *J. Catal.* 25, 273 (1972). This work was done for ammoxidation of propylene over a U/Sb catalyst. Similar results for oxidation of propylene to acrylonitrile over Bi/Mo catalysts have been found [see Ref. (2*g*)].

10. Trifiro, F., Centola, P., Pasquon, I., and Jiru, P., *Proc. Int. Congr. Catal. 4th 1968*, 310 (Paper 18); Trifiro, F., and Pasquon, I., *J. Catal.* 12, 412 (1968).